Dual Acute Proinflammatory and Antifibrotic Pulmonary Effects of Short Palate, Lung, and Nasal Epithelium Clone–1 after Exposure to Carbon Nanotubes

Y. Peter Di[1], Alexey V. Tkach[2], Naveena Yanamala[2], Shyla Stanley[2,3], Shengli Gao[1], Michael R. Shurin[4], Elena R. Kisin[2], Valerian E. Kagan[1], and Anna Shvedova[2,3]

[1]Department of Environmental and Occupational Health, University of Pittsburgh, Pittsburgh, Pennsylvania; [2]Pathology and Physiology Research Branch, National Institute of Occupational and Safety Health/Center for Disease Control and Prevention, Morgantown, West Virginia; [3]Department of Physiology and Pharmacology, West Virginia University, Morgantown, West Virginia; and [4]Department of Pathology, University of Pittsburgh Medical Center, Pittsburgh, Pennsylvania

Carbon nanotubes (CNTs; allotropes of carbon with a cylindrical nanostructure) have emerged as one of the most commonly used types of nanomaterials, with numerous applications in industry and biomedicine. However, the inhalation of CNTs has been shown to elicit pulmonary toxicity, accompanied by a robust inflammatory response with an early-onset fibrotic phase. Epithelial host-defense proteins represent an important component of the pulmonary innate immune response to foreign inhalants such as particles and bacteria. The short palate, lung, and nasal epithelium clone–1 (SPLUNC1) protein, a member of the bactericidal/permeability-increasing–fold (BPIF)–containing protein family, is a 25-kD secretory protein that is expressed in nasal, oropharyngeal, and lung epithelia, and has been shown to have multiple functions, including antimicrobial and chemotactic activities, as well as surfactant properties. This study sought to assess the importance of SPLUNC1-mediated pulmonary responses in airway epithelial secretions, and to explore the biological relevance of SPLUNC1 to inhaled particles in a single-walled carbon nanotube (SWCNT) model. Using *Scgb1a1-hSPLUNC1* transgenic mice, we observed that SPLUNC1 significantly modified host inflammatory responses by increasing leukocyte recruitment and enhancing phagocytic activity. Furthermore, we found that transgenic mice were more susceptible to SWCNT exposure at the acute phase, but showed resistance against lung fibrogenesis through pathological changes in the long term. The binding of SPLUNC1 also attenuated SWCNT-induced TNF-α secretion by RAW 264.7 macrophages. Taken together, our data indicate that SPLUNC1 is an important component of mucosal innate immune defense against pulmonary inhaled particles.

Keywords: SPLUNC1; BPIFA1; carbon nanotube; fibrosis; inflammation

CLINICAL RELEVANCE

This study provides a better understanding of airway epithelial defenses against inhaled environmental particles, including nanoparticles. This knowledge will likely help improve strategies to alleviate respiratory nanotoxicity in the future.

The advancement of nanotechnology presents many opportunities and benefits for new materials with significantly improved properties, as well as revolutionary applications in the fields, for example, of electronics, energy, environment, biomaterials, and medicine (1). Single-walled carbon nanotubes (SWCNTs; allotropes of carbon with a cylindrical nanostructure) have emerged as one of the most commonly used types of nanomaterials, with numerous applications in industry and biomedicine. SWCNTs have a diameter of only approximately 1 nanometer, but their length can be more than a million times greater. Although SWCNTs are versatile and beneficial in various applications, the inhalation of these nanoparticles exerts negative effects on the normal physiological functions of lungs, and causes pulmonary toxicity (2–5). We previously demonstrated that the pharyngeal aspiration of SWCNTs elicits pulmonary effects in C57BL/6 mice, with a combination of robust, acute inflammation and early-onset yet progressive fibrosis and granulomas (2, 5, 6). The early phase of lung innate immune responses to SWCNTs is characterized by inflammation mediated by phagocytic cells, namely, polymorphonuclear leukocytes (PMNs) and alveolar macrophages (AMs) (7).

The conducting airway serves as the first line of protection against environmental insults and pathogens, and as a barrier that prevents potentially injurious materials and infectious agents from entering the body (8). Airway secretion from epithelial cells and the mucus layers plays an important role in the defense against inhaled particles, including carbon nanotubes (CNTs) (9). These epithelial cell–mediated protections are complemented by mucociliary clearance and mucosal immunity, for instance in effects on the influx of inflammatory cells and on innate and acquired immune responses. One of the major airway secretory proteins, the palate, lung, and nasal epithelium clones (PLUNC), is highly expressed in the mouth, nose, and upper airways of humans and other vertebrate animals (10).

Originally named PLUNC (11), the gene product now called SPLUNC1 (short PLUNC1) is also referred to as secretory protein in upper respiratory tract (12), lung-specific X protein (13), nasopharyngeal carcinoma-related protein (14), or bactericidal/permeability-increasing–fold containing (BPIF) A1 protein (15). SPLUNC1 encodes a richly secreted protein detected in human sputum and tracheobronchial secretions, as well as in saliva (16), nasal lavage fluid (17), and apical secretions from cultured human tracheobronchial epithelial cells (11, 12, 18). SPLUNC1 and related PLUNC family members belong to

(*Received in original form October 29, 2012 and in final form May 5, 2013*)

This work was supported by National Institute of Occupational and Safety Health grants (NIOSH) - 3927ZKNL & 2927ZKCY (A.S.), National Institutes of Health grants R01 HL-091938 (Y.P.D.), ES-019304, HL-070755, and U19 AI-068021 (V.E.K.), and by the University of Pittsburgh Central Research Development Fund (Y.P.D.).

Correspondence and requests for reprints should be addressed to Y. Peter Di, Ph.D., Department of Environmental and Occupational Health, University of Pittsburgh, 100 Technology Drive, Suite 322, Bridgeside Point, Pittsburgh, PA 15219. E-mail: peterdi@pitt.edu; or Anna Shvedova, Ph.D., Pathology and Physiology Research Branch, National Institute of Occupational and Safety Health/Center for Disease Control and Prevention, Morgantown, WV 26505. E-mail: peterdi@pitt.edu or ats1@cdc.gov

This article has an online supplement, which is accessible from this issue's table of contents at www.atsjournals.org

Am J Respir Cell Mol Biol Vol 49, Iss. 5, pp 759–767, Nov 2013

Originally Published in Press as DOI: 10.1165/rcmb.2012-0435OC on May 30, 2013
Internet address: www.atsjournals.org

a larger protein family known as the BPIF proteins. SPLUNC1 is structurally similar to two BPIF family members with demonstrated innate immune roles, namely, BPI and lipopolysaccharide-binding protein (19–21). Notably, our proteomics data demonstrated the overexpression of SPLUNC1 in the lungs of mice after repeated exposures to SWCNTs (22). SPLUNC1 is one of the most abundantly secreted proteins from the airway epithelium, but its functional role during the inhalation of particles has never been examined.

SPLUNC1 exerts antimicrobial activity, and mice overexpressing SPLUNC1 exhibit enhanced protection against *Pseudomonas aeruginosa* and *Mycoplasma pneumoniae* (23, 24). SPLUNC1 has also been reported to bind the Gram-negative bacteria cell wall component LPS (25, 26). Moreover, SPLUNC1 may be required to regulate certain physical properties of airway surface liquid that are critical for proper mucociliary clearance in the lung, including airway surface liquid volume (27, 28) and surface tension (29–31). We recently demonstrated that SPLUNC1 exhibits a chemotactic property that recruits leukocytes in helping with the clearance of bacteria (25). Although the protective functions of SPLUNC1 are likely realized through several, if not all, of these mechanisms, experimental analyses of the specific pathways involved in the responses to microbial pathogens are obscured by the multiplicity of possible targets. An interesting opportunity to dissect the mechanisms triggered by SPLUNC1 may be offered by using chemically well-defined SWCNTs as a challenge to induce a robust inflammatory/immune response, uncomplicated by interactions with complex microbial surfaces.

In this study, we used a well-characterized mouse model of SWCNT pharyngeal aspiration to study the possible protective functions of SPLUNC1 in the lung, using gain-of-function approaches achieved through an overexpression of SPLUNC1 in genetically modified transgenic (TG) mice. We report that *Scgb1a1-hSPLUNC1* TG mice exhibit enhanced PMN recruitment and activation relative to those of their wild-type (WT) littermates durig the initial acute phase of the inflammatory response, followed by attenuated lung-tissue remodeling and fibrosis. Furthermore, using molecular modeling experiments, we show that the SPLUNC1 coating on SWCNT surfaces (mediated via hydrophobic interactions) may be responsible for the observed differential outcomes in cellular and biological responses between *Scgb1a1-hSPLUNC1* TG mice and their WT littermates.

MATERIALS AND METHODS

Animal Husbandry

Scgb1a1-hSPLUNC1 transgene mice constitutively express human SPLUNC1 (hSPLUNC1) protein in the mouse respiratory epithelium, and have been previously described (23). The genetic background of *Scgb1a1-hSPLUNC1* transgene mice and their WT littermates is FVB/N. Mice were maintained under specific pathogen–free conditions, with 12-hour light/dark cycles. All procedures were performed using mice at 7–10 weeks of age, maintained at the University of Pittsburgh in ventilated microisolator cages housed in animal facilities accredited by the American Association for Accreditation of Laboratory Animal Care. Protocols and experiments involving animals were performed in accordance with National Institutes of Health (32) guidelines, and approved by the Institutional Animal Care and Use Committee at the University of Pittsburgh.

Preparation of SWCNT Particles

The chemical cutting of SWCNTs was performed as reported previously (3, 33, 34) to obtain short SWCNTs ($\sim$ 200 nm in length). Briefly, the nanotubes were dispersed in a 3:1 mixture of concentrated H_2SO_4 and HNO_3, and sonicated in an ultrasonic bath using an output power of 70 W at 40 KHz in a Branson 1510 Sonifier (Branson Untrasonics, Danbury, CT) for 3 hours at 40°C. This solution was then diluted 10-fold by deionized water and filtered through polytetrafluoroethylene membrane (0.2 μm, 25 mm; SterliTech, Kent, WA). This collected sample was thoroughly washed with deionized water until a neutral pH was achieved, and the sample was then vacuum-dried at 110°C for 30 minutes. The short nanotubes thus obtained were dispersed in 25 mM HEPES buffer (pH 7.4; containing 150 mM NaCl) by sonication. Stock concentrations were further diluted to obtain the required concentrations in PBS buffer (pH 7.0). The prepared solutions were further sterilized and sonicated (three 1-min cycles) immediately before use.

Animal Exposure to SWCNTs

Pharyngeal aspiration was used to introduce SWCNTs to the mouse lung. In brief, after anesthesia with a mixture of ketamine and xylazine (62.5 and 2.5 mg/kg, subcutaneously in the abdominal area; Phoenix, St. Joseph, MO), the mouse was placed on a board in a near-vertical position, and the tongue was gently extended with lined forceps. A suspension of SWCNTs (80 μg/mouse; 60 μl in PBS) was placed posteriorly in the throat, and the tongue was held until the suspension was aspirated into the lungs. Particles were sterilized before administration by autoclaving the particle suspension.

Data Analysis

Statistical comparisons between cohorts were performed using ANOVA. A Dunnett multiple-comparisons test (one-way ANOVA) was used for comparisons of two differently treated groups with the control group, as well as for comparisons of SPLUNC1 TG treated mice versus WT treated mice (Figures 1 and 3–6). The Bonferroni multiple-comparisons test (two-way ANOVA) was used for performing multiple-comparison tests between the two differently treated groups at all time points investigated (Figure 2). $P < 0.05$ was considered statistically significant.

RESULTS

Enhanced Leukocyte Recruitment in SPLUNC1 TG Mice

We had previously generated a TG mouse model (*Scgb1a1*-hSPLUNC1) in which hSPLUNC1 was highly expressed in the airway epithelium. These TG mice exhibited more enhanced antibacterial activity than their WT littermates (23). We also recently reported that recombinant human SPLUNC1 protein (rSPLUNC1) displayed chemotactic properties in recruiting neutrophils and macrophages *in vitro* (25). To explore whether this chemotactic function is relevant in a more biological setting, we examined the effects of SPLUNC1 overexpression in modulating the host response to SWCNTs *in vivo*, using the established TG animal model. One day after pulmonary exposure to SWCNTs, we observed a significant increase ($\sim$ 3-fold, $P < 0.05$) of neutrophils in *Scgb1a1*-hSPLUNC1 TG mice, compared with those of their WT littermates (Figure 1A). No significant increase in AM recruitment was observed immediately after SWCNT exposure, but a slight increase of AMs in TG mice was evident at 28 days after exposure, compared with the AMs of their WT littermates (Figure 1B). The observed increase of leukocytes was consistent with the proposed function of SPLUNC1 in enhancing the recruitment of phagocytic cells to remove foreign particles such as bacteria and SWCNTs.

Pulmonary Damage after SWCNT Exposure

We observed increased total protein concentrations in the bronchoalveolar lavage (BAL) of TG mice compared with their WT littermates at 1 day after SWCNT exposure (Figure 2A). The increased total protein, and especially the amount of lactate dehydrogenase (LDH; an indicator of lung-tissue breakdown), suggested that the enhanced leukocyte recruitment in TG mice

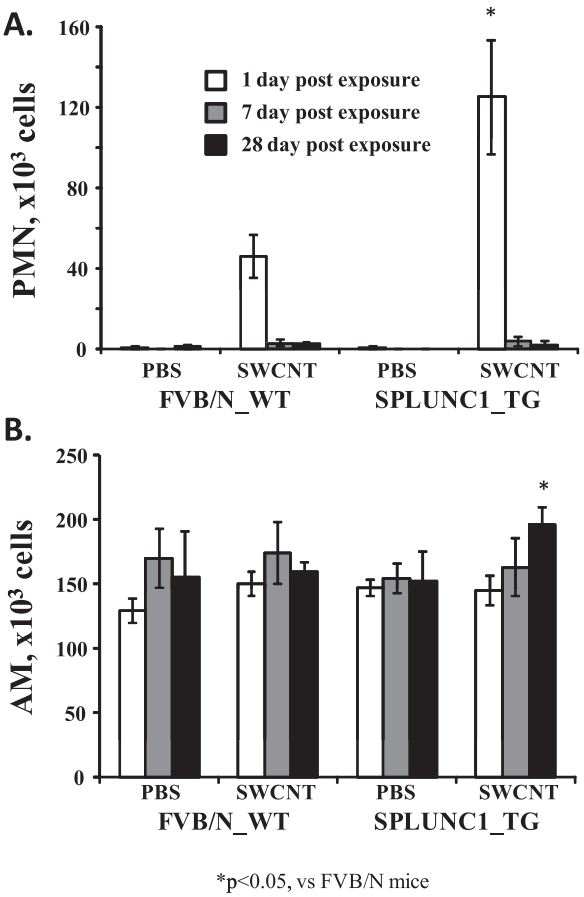

Figure 1. *Scgb1a1-hSPLUNC1* transgenic (TG) mice show increased inflammatory-cell recruitment after single-walled carbon nanotube (SWCNT) exposure. *Scgb1a1-hSPLUNC1* TG and wild-type (WT) mice were instilled with SWCNTs. At 1, 7, or 28 days after instillation, the lungs were lavaged, and a manual differential cell count was determined on bronchoalveolar lavage fluid (BALF) cytospin slides. Both neutrophil (*A*; 1 d) and macrophage (*B*; 28 d) counts were significantly higher in TG mice after challenge. Results represent the means ± SEMs from two independent experiments ($n = 5$ mice for each group). *$P <$ 0.05 for TG to WT comparisons at each time point. AM, alveolar macrophages; PMN, polymorphonuclear leukocytes.

may have been accompanied by more severe pulmonary damage in TG mice than in their WT counterparts at 1 day after SWCNT instillation (Figure 2B). The administered SWCNTs did not result in mortality in any mice, and both the WT and TG groups of mice recovered efficiently from the exposure-induced pulmonary injury. The difference in acute pulmonary injury between WT and TG mice disappeared during the recovery period, in regard to their concentrations of total protein (at 7 d after exposure) and LDH (at 28 d after exposure).

Increased Proinflammatory Cytokine Production in TG Mice after SWCNT Challenge

A proinflammatory pattern of pulmonary cytokine release was found on Days 1 and 7 after SWCNT exposure in both TG and WT animals (Figures 2C and 2D). Notably, the magnitudes of secretion for both TNF-α and IL-6 were consistently higher in BAL fluid (BALF) from TG mice, compared with those from WT mice (Figures 2C and 2D). The concentrations of IL-10, IL-12p70, IFN-γ, and monocyte chemotactic protein–1 had not significantly changed in SWCNT-exposed mice, compared with those of the control mice. The differences in proinflammatory cytokine secretion between TG and WT mice disappeared at 28 days after SWCNT exposure (Figures 2C and 2D).

SPLUNC1 Expression Protected Mouse Lungs from SWCNT-Induced Fibrosis

Greater pulmonary damage was observed in *Scgb1a1*-SPLUNC1 TG mice during the acute phase after SWCNT instillation (Day 1) compared with their WT counterparts, as evidenced by LDH and protein accumulations in BALF. At 7 days after SWCNT exposure, the difference between TG and WT mice in terms of pulmonary damage was much smaller than the difference at the earlier time point, 1 day after exposure (Figure 2). Nonetheless, a morphometric analysis of mouse lungs on Day 28 after exposure revealed that SWCNT administration resulted in significant interstitial pulmonary fibrosis in WT animals. Notably, in SWCNT-exposed WT mice, the average alveolar wall thickness was 6.72 ± 0.21 μm (versus 5.86 ± 0.2 μm in nonexposed WT control mice, $P < 0.05$), whereas in *Scgb1a1*-SPLUNC1 TG mice, alveolar wall thickness (6.0 ± 0.12 μm) was similar to that in nonexposed TG control mice (5.76 ± 0.11 μm). The net increase in the thickness of the alveolar walls was thus significantly greater in WT mice (0.86 ± 0.21 μm; Figures 3B and 3D) compared with that in TG mice (0.24 ± 0.12 μm; Figures 3C and 3E). In addition, the concentration of transforming growth factor–β1 measured on Day 28 after exposure to SWCNT pharyngeal aspiration was significantly higher in the BAL of WT mice than in TG mice (Figure 3F). These data suggest that SPLUNC1 expression protected the mouse lung from SWCNT-induced fibrosis.

SPLUNC1 Targets SWCNTs to AMs

To evaluate SWCNT capture (potential clearance) by AMs in the lung, we counted the number of AMs containing particulate inclusions in BALF. In WT mice, 32% ± 5% of BAL macrophages were found to contain SWCNT inclusions at 24 hours after exposure (Figure 4A). In contrast, 59% ± 6% of AMs in SPLUNC1 TG mice contained SWCNTs. This difference persisted until 7 days after SWCNT treatment, insofar as AMs from TG mice maintained a continuously and significantly higher engulfment of SWCNTs than did the AMs from WT mice (Figure 4; 35% ± 3% versus 21% ± 2%, respectively; $P < 0.05$). Thus, the presence of SPLUNC1 within the lung facilitated the capture of SWCNTs by AMs. To evaluate further whether interstitial macrophages in TG mice similarly exhibited a more efficient engulfment of SWCNTs, lung-tissue sections from SWCNT-exposed mice were examined, and interstitial AMs containing SWCNTs were tallied. The average percentage of interstitial AMs with SWCNTs in TG mice was more than threefold higher than the percentage of AMs from WT mice at 7 days after SWCNT exposure (Figure 5; 14.1% ± 3.1% versus 4.5% ± 0.9%, respectively; $P < 0.05$). The significantly higher percentage of interstitial AMs with SWCNTs in TG mice (i.e., 2-fold) continued even at 28 days after the initial SWCNT exposure (Figure 5; 10.8% ± 2.9% versus 5.1% ± 1.9%, respectively; $P < 0.05$).

To evaluate further the enhanced clearance of SWCNTs and the targeting of SWCNTs to AMs by SPLUNC1, we examined lung-tissue sections of WT and TG mice 7 days after SWCNT exposure, using enhanced dark-field microscopy. The distribution of SWCNTs in the lungs was quantified using standard morphometric grid point counting methods, as previously described (35). Evaluated counting categories included points over SWCNTs in the (*1*) alveolar airspace region, (*2*) AMs, and (*3*) alveolar tissue region. The fractional distribution of particles in each category per animal for the two groups is shown in Table 1.

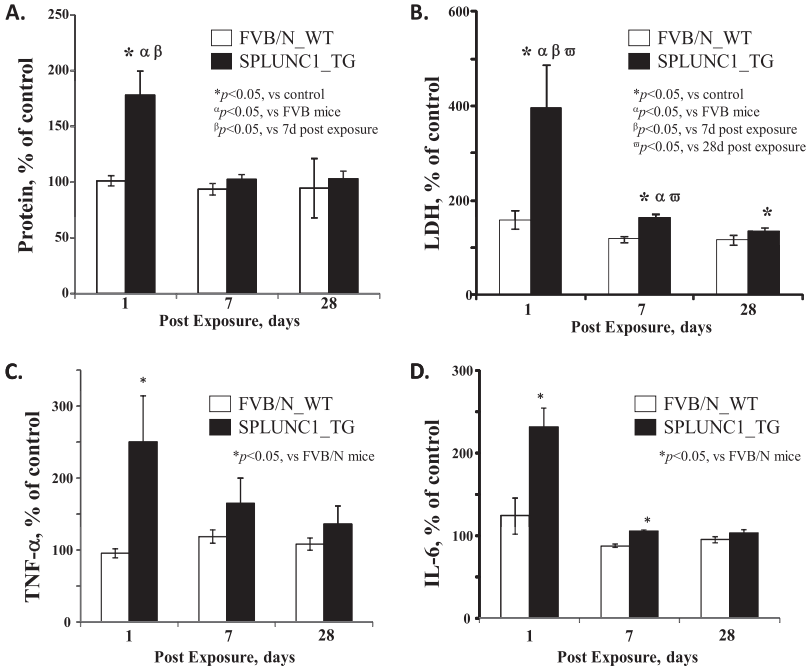

Figure 2. *Scgb1a1-hSPLUNC1* transgenic mice exhibit increased pulmonary damage and proinflammatory cytokine production during the acute phase after SWCNT exposure. *Scgb1a1-hSPLUNC1* TG mice and WT littermate control mice were instilled with 80 μg SWCNTs per mouse. Total protein, lactate dehydrogenase (LDH), and cytokine concentrations in BALF were determined at the indicated recovery time points. *Scgb1a1-hSPLUNC1* TG mice exhibited significantly increased concentrations of total protein (*A*), LDH (*B*), and proinflammatory cytokines TNF-α (*C*) and IL-6 (*D*) in BALF. Results represent the means ± SEMs from two independent experiments (n = 5 mice for each group). *$P < 0.05$, $^{\alpha}P < 0.05$, $^{\beta}P < 0.05$, and $^{\omega}P < 0.05$, for TG to WT comparisons at each time point. d, days; SPLUNC1, short palate, lung, and nasal epithelium clone–1.

The total SWCNT content (total percentage of fractional distribution of particles in all categories) in the lungs of WT mice was markedly higher (∼ 4.30%) than in TG mice (∼ 2.49%). This effect was largely attributable to the higher SWCNT concentrations in the alveolar tissue (3.37 times) and alveolar airspace (3.50 times) of WT mice versus SPLUNC1 TG mice. In contrast, the SWCNT content was elevated (∼ 1.90-fold) in AMs of *Scgb1a1*-SPLUNC1 TG mice, compared with that of WT animals.

SPLUNC1 Inhibits SWCNT-Induced TNF-α Secretion

TNF-α is a key inflammatory cytokine secreted from macrophages in response to stimulation by LPS. We observed a dose-dependent increase in TNF-α secretion when mouse leukaemic monocyte macrophage (RAW 264.7) cells were stimulated with SWCNTs. Interestingly, the preincubation of SWCNTs with rSPLUNC1 inhibited SWCNT-induced TNF-α secretion by approximately 50%. These results suggest that SPLUNC1 possesses anti-inflammatory activity (Figure 6).

Molecular Modeling of the Interaction between SWCNT and SPLUNC1

Computer modeling was used to further our understanding of molecular interactions and characterize the putative SWCNT binding sites in SPLUNC1. The predicted docking of the pristine and two differently oxidatively modified SWCNTs, as described previously by Kagan and colleagues (3), to the structural model of SPLUNC1, using the Autodock Vina program (36), resulted

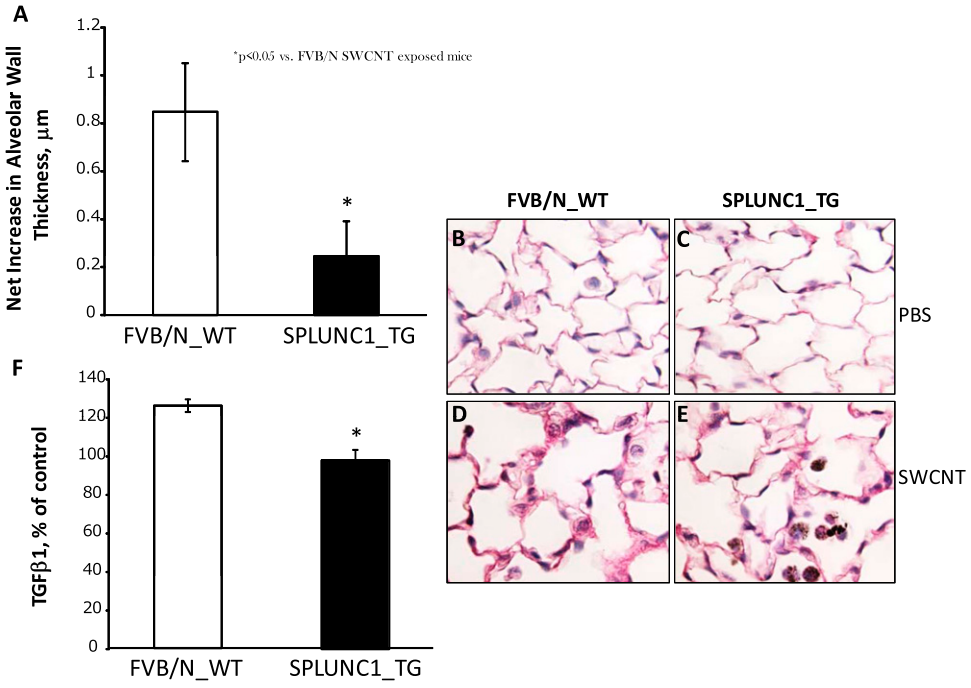

Figure 3. Alleviated alveolar wall thickening in *Scgb1a1-hSPLUNC1* transgenic mice after SWCNT challenge. Morphometric changes were ascertained in the connective tissue of alveolar wall regions from lung sections of TG and WT mice in response to SWCNTs at 28 days after pharyngeal aspiration. (*A*) The net increase in alveolar wall thickness in TG mice is significantly less than that of WT mice. (*B* and *C*) Sirius red–stained lung sections of WT (*B*) or TG (*C*) mice 28 days after aspiration of PBS (control mice). (*D* and *E*) Sirius red–stained lung sections of WT (*D*) or TG (*E*) mice at 28 days after aspiration of 80 μg SWCNTs/mouse. (*F*) Transforming growth factor–β1 (TGF-β1), measured in the BALF of mice on Day 28 after pharyngeal aspiration with SWCNTs, exhibited at a significantly lower concentration in TG mice than in WT mice. Values represent means ± SEMs (n = 5 mice/group). *$P < 0.05$, for TG versus SWCNT-treated WT mice.

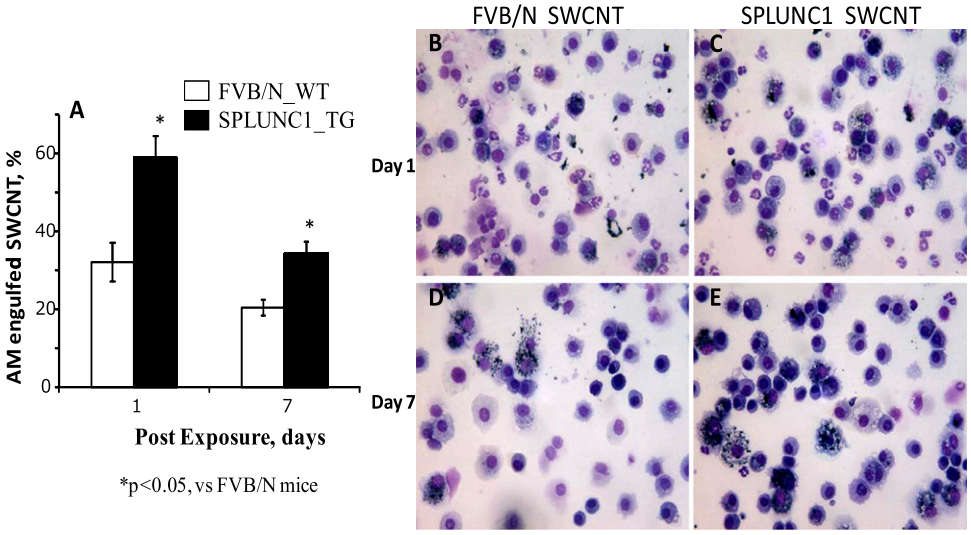

Figure 4. Enhanced alveolar macrophage engulfment of SWCNTs in *Scgb1a1-hSPLUNC1* transgenic mice after challenge. (*A*) BAL cells were recovered from lungs of WT or TG mice on Days 1 and 7 after SWCNT exposure. Quantitated results of BAL macrophages with SWCNTs are presented. (*B–E*) BAL cells, 1 day (*B* and *C*) and 7 days (*D* and *E*) after exposure to SWCNTs. Results represent the means ± SEMs from two independent experiments ($n = 5$ mice for each group). *$P < 0.05$, for TG to WT comparisons at each time point.

in different binding sites in SPLUNC1 (Figure 7). In all cases, they were found to localize to a common single binding site in SPLUNC1 (Figure 7A, labeled as Site 1). In addition, a second binding site, labeled Site 2, located on the opposite side from Site 1, was also predicted to be one of the possible binding sites for oxidized SWCNTs (Figures 7A and 7C). However, the lowest energy conformation in all cases was predicted to be at Binding Site 1 (Table 2). The interactions of SWCNTs at this site are predicted to be stabilized by a set of residues involving Leu24, Pro27, Leu28, Pro32, Ile92, Asn95, Ile96, Pro97, Leu98, Leu99, Pro247, Leu248, Gly251, and Ile252 (Figure 7B and Table 2). Because more than 90% of the residue is hydrophobic at Binding Site 1, it is likely that the binding of SWCNTs in SPLUNC1 is stabilized by hydrophobic interactions. This is further supported by the lack of electrostatic interactions between the oxidized groups in SWCNTs and the positively charged residue in SPLUNC1 at both predicted binding sites (Table 2). In addition, the oxidized groups on SWCNTs are oriented toward the aqueous phase, away from the SPLUNC1 binding sites. SPLUNC1 belongs to the BPI fold–containing family of proteins, and has a relatively high grand average of hydropathicity index at 0.634 (mouse) and 0.608 (human), which clearly classifies SPLUNC1 as a hydrophobic protein similar to surfactant proteins (29). Together, these results indicate that the binding of nonoxidized/oxidized SWCNTs at Site 1 is preferable to binding at Site 2 and is dominated by hydrophobic interactions. Thus, the selective binding of SPLUNC1 on the SWCNT surface via hydrophobic interactions (Figure 7D) leads to SPLUNC1-coated SWCNTs, and likely influences their uptake, clearance, and distribution, compared with those of uncoated SWCNTs *in vivo*.

DISCUSSION

The goal of this study was to investigate the biological roles of SPLUNC1's chemotactic and anti-inflammatory activity in airway epithelial secretions *in vitro* and *in vivo*. We intended to address two questions in this study. First, does chemotactic activity, demonstrated by native SPLUNC1 and observed *in vitro*, also help recruit leukocytes to the alveolar region during lung

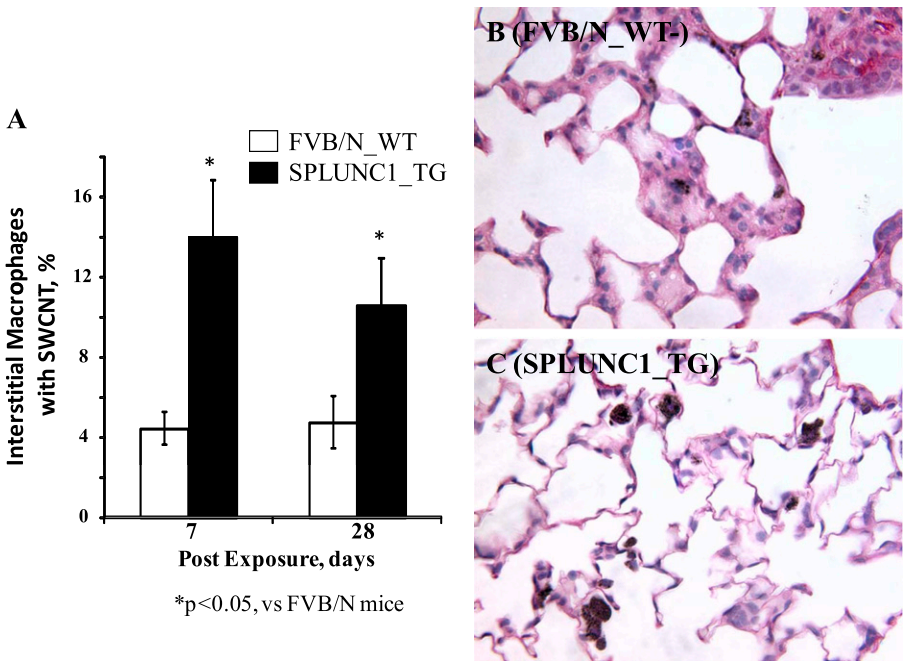

Figure 5. Pulmonary macrophages in lung sections of transgenic or wild-type mice at 7 days after SWCNT exposure. (*A*) Quantitated results of lung alveolar macrophages with SWCNTs. Histopathologic images of lung sections are representative of WT (*B*) or TG (*C*) mice exposed to SWCNTs (7 d after treatment). Values represent means ± SEMs ($n = 5$ mice/group). *$P < 0.05$, for TG versus SWCNT-treated WT mice.

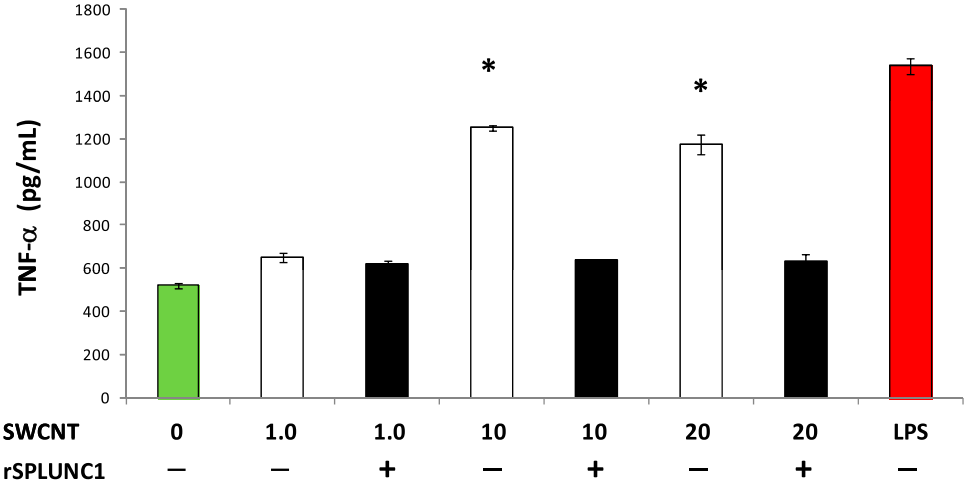

Figure 6. SPLUNC1-inhibited, SWCNT-induced TNF-α release by RAW 264.7 macrophages. RAW 264.7 cells (5×10^4/well) were incubated with LPS (1 μg/ml) and SWCNTs (1–20 μg/ml), with or without preincubation with recombinant human SPLUNC1 (rSPLUNC1; 30 μg/ml) for 18 hours. The secretion in culture media was assayed for TNF-α ($P \leq 0.05$). Values represent the means ± SEMs of three independent experiments. *Different from secretion in the presence of rSPLUNC1, $P < 0.05$.

injury and clear SWCNTs? Second, does SPLUNC1 exert direct anti-inflammatory activity in modulating pulmonary immune responses? Our data indicate that excessive SPLUNC1 and the resulting leukocyte recruitment caused initial pulmonary damage and higher proinflammatory cytokine secretion during the acute phase after SWCNT exposure. During the chronic phase at 28 days after SWCNT exposure, however, the anti-inflammatory activity of SPLUNC1 conversely helped alleviate the pulmonary fibrosis, one of the hallmark negative outcomes of SWCNT exposure.

Our investigation into the SPLUNC1 modulation of host responses to SWCNT builds on earlier studies indicating that SPLUNC1 may possess both chemotactic and anti-inflammatory activities, two functions that normally produce opposite outcomes (23, 25). During the initial stage of a bacterial infection, increased SPLUNC1 expression not only exhibits antimicrobial activity to control bacterial numbers, but also recruits phagocytic cells such as neutrophils and macrophages to assist in the clearance of bacteria. Subsequently, the anti-inflammatory activity of SPLUNC1 helps resolve leukocyte-induced inflammation and protects the host from unwanted lung tissue damage. Because instilled bacteria in the mouse lung can still multiply, the total number of inflammatory cells may be affected by bacterial burden, rather than reflecting bona fide chemotactic activity. Chemically well-defined SWCNTs trigger "sterile" inflammation uncomplicated by the possible antimicrobial activity of SPLUNC1, its diverse interactions with multifaceted microbial surfaces, and the effects of bacterial pathogens on cells of the innate immune system. The use of SWCNTs also provides an opportunity to investigate the potential interactions between SPLUNC1 and inhaled foreign particles.

To better understand the contributions of SPLUNC1 function to airway host defense against inhaled particles, we compared the susceptibility of SPLUNC1 TG mice and WT littermates, using a SWCNT exposure model. Our previously published proteomics data demonstrated the overexpression of SPLUNC1 in the lungs of mice after repeated exposures to SWCNTs (32), suggesting that the up-regulation of SPLUNC1 is a feature of the innate immune response to environmental foreign particles. In the present study, an 80-μg bolus of SWCNTs per mouse was delivered by pharyngeal aspiration to the mice. This technique provides for the widespread delivery of particles throughout the lung at a single time point, using a pathophysiologically relevant concentration. Airborne concentrations of nanotubes were reported in several recent field studies to be as high as 430 $\mu g/m^3$ for multi-walled carbon nanotubes, and 53 $\mu g/m^3$ for SWCNTs (37–41). Therefore, the SWCNT dose used in the present study is relevant to actual workplace exposures, and is certainly lower than those exposures that could be achieved during a lifetime of work exposures (8 h/d, 5 d/wk, 45 yr) (http://www.cdc.gov/niosh/docket/archive/docket161A).

We have shown in previous studies that SPLUNC1 TG mice display enhanced bacterial clearance, which is accompanied by a decrease in neutrophil infiltration and cytokine concentrations after *in vivo P. aeruginosa* challenge (23). In contrast to the response after a bacterial infection, we found that the overexpressed SPLUNC1 showed a slightly different outcome in regard to its acute-phase response to SWCNT exposure. Because SPLUNC1-mediated antimicrobial activity did not contribute to controlling the numbers of SWCNTs, the enhanced recruitment of leukocytes by SPLUNC1 (Figure 1) resulted in the temporarily increased secretion of proinflammatory cytokines and pulmonary damage (Figure 2) during the acute phase after SWCNT exposure. Nonetheless, the anti-inflammatory activity of SPLUNC1 was still able to help alleviate long-term lung pathological changes, such as fibrosis (Figure 3).

The constitutively expressed SPLUNC1 in the TG mice with instilled SWCNTs was associated with increased leukocyte recruitment in mouse lungs and the enhanced capture of SWCNTs by AMs. Consistent with this hypothesis, we detected a significant increase in proinflammatory cytokine TNF-α and IL-6 concentrations in the BALF from SWCNT-exposed TG mice. Because

TABLE 1. LUNG DISTRIBUTION OF SWCNTS AT 7 DAYS AFTER EXPOSURE IN THE ALVEOLAR REGION OF SPLUNC1 TG AND WT MICE

	Alveolar Tissue	Alveolar Air Space	Alveolar MΦ	Total Particles	Percent MΦ with Engulfed SWCNTs
TG mice	0.82 ± 0.08	0.22 ± 0.09	1.46 ± 0.06	2.49 ± 0.08	87.74 ± 3.96
WT mice	2.76 ± 0.2	0.77 ± 0.02	0.77 ± 0.14	4.30 ± 0.33	90.0 ± 7.07

Definition of abbreviations: MΦ, macrophages; SPLUNC1, short palate, lung, and nasal epithelium clone–1; SWCNTs, single-walled carbon nanotubes; TG, transgenic; WT, wild-type.

Distribution of the SWCNT burden in the alveolar region of lungs, composed of tissue, airspace, and macrophages, is listed. The fractional distribution of each category is expressed as percentage per counting category. Data are presented as means ± SEMs for each category within a group.

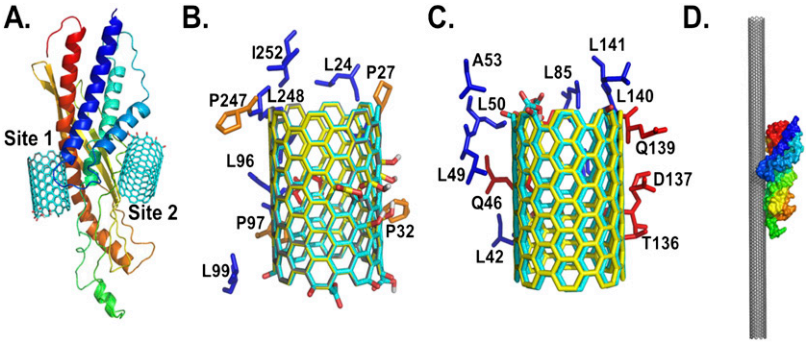

Figure 7. Structural details of the predicted binding sites of nonoxidized and oxidized SWCNTs on SPLUNC1. (*A*) Structural model of SPLUNC1, along with the two predicted binding sites 1 and 2, with oxidized SWCNTs at the ends. The residues that are within close proximity of SPLUNC1 (within 4 Å) stabilize the binding sites. Amino-acid compositions of the predicted Site 1 (*B*) and (*C*) Site 2 of SPLUNC1 interact with nonoxidized SWCNTs (*gray*), oxidize SWCNTs at the ends (*cyan*), and (*D*) oxidize SWCNTs in the middle (*yellow*). The predicted binding orientation of SPLUNC1 to a SWCNT surface is demonstrated in a 25-nm length. The structure of SPLUNC1 in *A* and *D* is rendered as cartoon and surface, respectively, and is colored as a rainbow from the N-terminus to the C-terminus. The proline, hydrophobic, and polar residues in *B* and *C* are colored in *orange*, *blue*, and *red*, respectively, and are rendered as *sticks*. A, alanine; D, aspartic acid; I, isoleucine; L, leucine; P, proline; Q, glutamine; T, threonine.

the amount of overexpressed SPLUNC1 was significantly higher than the increased amount of SWCNT-induced mouse SPLUNC1, naturally induced SPLUNC1, at a lower expression level than that of genetically overexpressed SPLUNC1, may not cause such a significant increase in leukocyte recruitment and pulmonary damage, but may still maintain the beneficial effects of the SPLUNC1-mediated clearance of SWCNTs and anti-inflammatory activity. Unfortunately, this potential dosage effect of SPLUNC1-mediated pulmonary defense was not testable using the constitutively expressed SPLUNC1 TG mouse model that is currently available.

This study provides direct *in vivo* evidence that SPLUNC1 possesses chemotactic activity in the context of environmental particle exposure with a SWCNT model. Our investigation into the anti-inflammatory responses of SPLUNC1 both *in vitro* and *in vivo* suggests that increased SPLUNC1 likely contributes to the decreased inflammation in TG mice during fibrogenesis. The discrepancy in TNF-α responses between *in vivo* and *in vitro* studies may correspond to two different scenarios, and is possibly relevant to a timing effect *in vivo*. The early TNF-α response found *in vivo* (Figure 2C) is associated with increased leukocyte recruitment during the initial acute phase of inflammatory responses evoked by SWCNT administration (Figure 1). The suppression of TNF-α production (Figure 6) by stimulated macrophages incubated in the presence of SPLUNC1 *in vitro* may correspond to the *in vivo* anti-inflammatory activity of SPLUNC1 at a later stage (chronic phase) directed toward macrophages. These diverse effects of SPLUNC1 in modulating innate immune responses are compatible with its role in the recruitment of leukocytes during the acute phase of inflammation, followed by its ability to restrain the magnitude of the chronic-phase proinflammatory responses of macrophages. However, the direct activation of macrophages by SWCNTs to stimulate proinflammatory cytokine TNF-α expression has not been previously demonstrated. Although it remains unclear whether SWCNT-mediated macrophage activation is receptor-dependent, the potential binding of hydrophobic SPLUNC1 to SWCNTs may have prevented the SWCNT-induced activation of macrophages to trigger inflammatory responses (Figure 6). This is further supported by our molecular modeling experiments, which indicated that the hydrophobic interaction between SPLUNC1 and SWCNTs can lead to the coating of SPLUNC1 on the SWCNT surface, masking the nascent nanoparticle.

Protein-coated particles have been shown to be nontoxic or less toxic, compared with uncoated particles (42). The coating of SPLUNC1 on the surface of SWCNTs could lead to altered cellular interaction pathways and result in attenuated cytotoxic effects. This is in line with the experimental data, where an increased engulfment of SWCNTs by AMs was observed in SPLUNC1 TG mice (Figures 4 and 5). A recent study demonstrated that the presence of lung surfactant protein D, or the lipid coating around SWCNTs, significantly enhanced the uptake of SWCNTs by macrophages *in vitro* (43). In fact, protein-coated nanoparticles have been shown to interfere with biological

TABLE 2. PUTATIVE INTERACTION SITES OF NONOXIDIZED AND OXIDIZED SWCNTS ON SPLUNC1

	Binding Site 1		Binding Site 2	
Type of SWCNT	Predicted Energy (Number of Conformations)	5-Å Residues	Predicted Energy (Number of Conformations)	5-Å Residues
Nonoxidized (pristine)	−18.1 Kcal/mol (9/9)	Leu24, Pro27, Leu28, Pro32, Ile92, Asn95, Ile96, Pro97, Leu99, Pro247, Leu248, Gly251, and Ile252		
Oxidized at ends	−15.9 Kcal/mol (8/9)	Leu24, Pro27, Leu28, Pro32, Ile92, Asn95, Ile96, Pro97, Leu98, Leu99, Pro247, Leu248, Gly251, and Ile252	−14.9 Kcal/mol (1/9)	Leu42, Gln46, Leu49, Leu50, Ala53, Leu85, S86, Leu90, Glu94, Thr136, Asp137, Gln139, Leu140, and Leu141
Oxidized in the middle	−14.1 Kcal/mol (8/9)	Leu24, Pro27, Leu28, Pro32, Ile92, Asn95, Ile96, Pro97, Leu98, Leu99, Pro247, Leu248, Gly251, and Ile252	−13.4 Kcal/mol (1/9)	Leu42, Gln46, Leu49, Leu50, Ala53, Leu85, Ser86, Leu90, Glu94, Thr136, Asp137, Pro138, Gln139, Leu140, and Leu141

Definition of abbreviations: SPLUNC1, short palate, lung, and nasal epithelium clone–1; SWCNT, single-walled carbon nanotube.

A list of all residues that stabilize within 5 Å of the two predicted binding sites, along with the lowest binding energy and the total number of conformations observed, is detailed for each case.

responses, either by switching off the intended interactions or by switching on the cellular machineries, such as activating endocytosis or phagocytosis pathways (43–47).

Our assessments of the SWCNT content in different pulmonary compartments indicate that AMs in SPLUNC1 TG animals exhibited a higher SWCNT load than those in WT mice (Table 1). This is compatible with the SPLUNC1-enhanced phagocytosis of SWCNTs in TG animals. In contrast, the limited capacity of macrophages to engulf SWCNTs in TG animals is not a likely contributor to the higher total SWCNT concentrations in WT animals, compared with SPLUNC1 TG animals. Given that SWCNT-containing macrophages were present in approximately the same amounts in the lungs of WT and TG mice (Figure 1), a different, as yet unidentified factor could also be responsible for the markedly higher presence of SWCNTs in both the alveolar tissue and alveolar spaces of WT mice compared with TG mice, an effect that largely accounted for the total pulmonary quantitative abundance of SWCNTs in WT versus TG mice. However, because SPLUNC1 is an airway-secreted protein with multiple functions, other aspects of SPLUNC1 activity may also contribute to the clearance of SWCNTs. SPLUNC1 has been suggested to function as a surface active agent, with potent and dose-dependent surface tension–reducing activity (29). Although those previous experiments were performed *in vitro* with purified recombinant SPLUNC1, the overexpressed SPLUNC1 in our TG mice may also have contributed to the elimination of SWCNTs through SPLUNC1-enhanced mucociliary clearance *in vivo*. The enhanced clearance of SWCNTs could be attributable to either reduced overall surface tension in the mucous layer of lungs, or to the specific coating of SPLUNC1 on the surface of SWCNTs via hydrophobic interactions, as demonstrated by molecular modeling experiments (Figure 7), leading to the enhanced biocompatibility of these particles, as previously demonstrated (43, 48). Although it is beyond the scope of this study, to examine the biological effects of SWCNT exposure on SPLUNC1 null mice, when these mice become available, would be interesting.

In conclusion, we present evidence that the airway secretory protein SPLUNC1 plays a significant role in modulating SWCNT-induced innate immune response. Using genetically modified *Scgb1a1*-hSPLUNC1 mice, we found that the overexpression of SPLUNC1 results in an increased recruitment of leukocytes in the airways, along with an increased susceptibility to SWCNT exposure during the acute phase. However, the enhanced capture of SWCNTs through AMs by SPLUNC1, and the anti-inflammatory activity of SPLUNC1, prevented long-term lung-tissue damage and remodeling. Our animal studies allowed us to demonstrate both chemotactic and anti-inflammatory activities of SPLUNC1 *in vivo*. This study provides a better understanding of airway epithelial defenses against inhaled environmental particles, and this knowledge may help improve strategies to alleviate respiratory nanotoxicity in the future.

Author disclosures are available with the text of this article at www.atsjournals.org.

Acknowledgments: The authors thank Marissa Di for editorial assistance with the manuscript.

References

1. Shvedova AA, Kisin ER, Porter D, Schulte P, Kagan VE, Fadeel B, Castranova V. Mechanisms of pulmonary toxicity and medical applications of carbon nanotubes: two faces of Janus? *Pharmacol Ther* 2009;121:192–204.
2. Shvedova AA, Kapralov AA, Feng WH, Kisin ER, Murray AR, Mercer RR, St Croix CM, Lang MA, Watkins SC, Konduru NV, *et al*. Impaired clearance and enhanced pulmonary inflammatory/fibrotic response to carbon nanotubes in myeloperoxidase-deficient mice. *PLoS ONE* 2012;7:e30923.
3. Kagan VE, Konduru NV, Feng W, Allen BL, Conroy J, Volkov Y, Vlasova II, Belikova NA, Yanamala N, Kapralov A, *et al*. Carbon nanotubes degraded by neutrophil myeloperoxidase induce less pulmonary inflammation. *Nat Nanotechnol* 2010;5:354–359.
4. Shvedova AA, Kagan VE. The role of nanotoxicology in realizing the "helping without harm" paradigm of nanomedicine: lessons from studies of pulmonary effects of single-walled carbon nanotubes. *J Intern Med* 2010;267:106–118.
5. Shvedova AA, Kisin ER, Mercer R, Murray AR, Johnson VJ, Potapovich AI, Tyurina YY, Gorelik O, Arepalli S, Schwegler-Berry D, *et al*. Unusual inflammatory and fibrogenic pulmonary responses to single-walled carbon nanotubes in mice. *Am J Physiol Lung Cell Mol Physiol* 2005;289:L698–L708.
6. Shvedova AA, Kisin E, Murray AR, Johnson VJ, Gorelik O, Arepalli S, Hubbs AF, Mercer RR, Keohavong P, Sussman N, *et al*. Inhalation vs. aspiration of single-walled carbon nanotubes in C57BL/6 mice: inflammation, fibrosis, oxidative stress, and mutagenesis. *Am J Physiol Lung Cell Mol Physiol* 2008;295:L552–L565.
7. Tkach AV, Shurin GV, Shurin MR, Kisin ER, Murray AR, Young SH, Star A, Fadeel B, Kagan VE, Shvedova AA. Direct effects of carbon nanotubes on dendritic cells induce immune suppression upon pulmonary exposure. *ACS Nano* 2011;5:5755–5762.
8. Tam A, Wadsworth S, Dorscheid D, Man SP, Sin DD. The airway epithelium: more than just a structural barrier. *Ther Adv Respir Dis* 2011;5;255–273.
9. Jachak A, Lai SK, Hida K, Suk JS, Markovic N, Biswal S, Breysse PN, Hanes J. Transport of metal oxide nanoparticles and single-walled carbon nanotubes in human mucus. *Nanotoxicology* 2012;6:614–622.
10. Di YP. Functional roles of SPLUNC1 in the innate immune response against Gram-negative bacteria. *Biochem Soc Trans* 2011;39:1051–1055.
11. Weston WM, LeClair EE, Trzyna W, McHugh KM, Nugent P, Lafferty CM, Ma L, Tuan RS, Greene RM. Differential display identification of PLUNC, a novel gene expressed in embryonic palate, nasal epithelium, and adult lung. *J Biol Chem* 1999;274:13698–13703.
12. Di YP, Harper R, Zhao Y, Pahlavan N, Finkbeiner W, Wu R. Molecular cloning and characterization of SPURT, a human novel gene that is retinoic acid–inducible and encodes a secretory protein specific in upper respiratory tracts. *J Biol Chem* 2003;278:1165–1173.
13. Iwao K, Watanabe T, Fujiwara Y, Takami K, Kodama K, Higashiyama M, Yokouchi H, Ozaki K, Monden M, Tanigami A. Isolation of a novel human lung–specific gene, LUNX, a potential molecular marker for detection of micrometastasis in non–small-cell lung cancer. *Int J Cancer* 2001;91:433–437.
14. Zhang BC, Zhu SG, Xiang JJ, Zhou M, Nie XM, Xiao BY, Li XL, Li GY. Analysis of splicing variants in NASG 3′UTR, down-regulated in nasopharyngeal carcinoma, and its expression in multiple cancer tissues [in Chinese]. *Ai Zheng* 2003;22:477–480.
15. Bingle L, Bingle CD. Distribution of human PLUNC/BPI fold–containing (BPIF) proteins. *Biochem Soc Trans* 2011;39:1023–1027.
16. Vitorino R, Lobo MJ, Ferrer-Correira AJ, Dubin JR, Tomer KB, Domingues PM, Amado FM. Identification of human whole saliva protein components using proteomics. *Proteomics* 2004;4:1109–1115.
17. Ghafouri B, Kihlstrom E, Stahlbom B, Tagesson C, Lindahl M. PLUNC (palate, lung and nasal epithelial clone) proteins in human nasal lavage fluid. *Biochem Soc Trans* 2003;31:810–814.
18. Campos MA, Abreu AR, Nlend MC, Cobas MA, Conner GE, Whitney PL. Purification and characterization of PLUNC from human tracheobronchial secretions. *Am J Respir Cell Mol Biol* 2004;30:184–192.
19. Bingle CD, Craven CJ. PLUNC: a novel family of candidate host defence proteins expressed in the upper airways and nasopharynx. *Hum Mol Genet* 2002;11:937–943.
20. Elsbach P, Weiss J. Role of the bactericidal/permeability-increasing protein in host defence. *Curr Opin Immunol* 1998;10:45–49.
21. Fenton MJ, Golenbock DT. LPS-binding proteins and receptors. *J Leukoc Biol* 1998;64:25–32.
22. Teeguarden JG, Webb-Robertson BJ, Waters KM, Murray AR, Kisin ER, Varnum SM, Jacobs JM, Pounds JG, Zanger RC, Shvedova AA. Comparative proteomics and pulmonary toxicity of instilled single-walled carbon nanotubes, crocidolite asbestos, and ultrafine carbon black in mice. *Toxicol Sci* 2011;120:123–135.

23. Lukinskiene L, Liu Y, Reynolds SD, Steele C, Stripp BR, Leikauf GD, Kolls JK, Di YP. Antimicrobial activity of PLUNC protects against *Pseudomonas aeruginosa* infection. *J Immunol* 2011;187:382–390.
24. Gally F, Di YP, Smith SK, Minor MN, Liu Y, Bratton DL, Frasch SC, Michels NM, Case SR, Chu HW. SPLUNC1 promotes lung innate defense against *Mycoplasma pneumoniae* infection in mice. *Am J Pathol* 2011;178:2159–2167.
25. Sayeed S, Nistico L, St. Croix C, Di YP. Multifunctional role of human SPLUNC1 in *Pseudomonas aeruginosa* infection. *Infect Immun* 2013; 81:285–291.
26. Ghafouri B, Kihlstrom E, Tagesson C, Lindahl M. PLUNC in human nasal lavage fluid: multiple isoforms that bind to lipopolysaccharide. *Biochim Biophys Acta* 2004;1699:57–63.
27. Garcia-Caballero A, Rasmussen JE, Gaillard E, Watson MJ, Olsen JC, Donaldson SH, Stutts MJ, Tarran R. SPLUNC1 regulates airway surface liquid volume by protecting ENAC from proteolytic cleavage. *Proc Natl Acad Sci USA* 2009;106:11412–11417.
28. Hobbs CA, Blanchard MG, Kellenberger S, Bencharit S, Cao R, Kesimer M, Walton WG, Redinbo MR, Stutts MJ, Tarran R. Identification of SPLUNC1's ENAC-inhibitory domain yields novel strategies to treat sodium hyperabsorption in cystic fibrosis airways. *FASEB J* 2012;26:4348–4359.
29. Gakhar L, Bartlett JA, Penterman J, Mizrachi D, Singh PK, Mallampalli RK, Ramaswamy S, McCray PB Jr. PLUNC is a novel airway surfactant protein with anti-biofilm activity. *PLoS ONE* 2010;5:e9098.
30. McGillivary G, Bakaletz LO. The multifunctional host defense peptide SPLUNC1 is critical for homeostasis of the mammalian upper airway. *PLoS ONE* 2010;5:e13224.
31. Liu Y, Bartlett JA, Di ME, Bomberger JM, Chan YR, Gakhar L, Mallampalli RK, McCray PB Jr, Di YP. SPLUNC1/BPIFA1 contributes to pulmonary host defense against *Klebsiella pneumoniae* respiratory infection. *Am J Pathol* 2013;182:1519–1531.
32. Duniho SM, Martin J, Forster JS, Cascio MB, Moran TS, Carpin LB, Sciuto AM. Acute changes in lung histopathology and bronchoalveolar lavage parameters in mice exposed to the choking agent gas phosgene. *Toxicol Pathol* 2002;30:339–349.
33. Allen BL, Kotchey GP, Chen Y, Yanamala NV, Klein-Seetharaman J, Kagan VE, Star A. Mechanistic investigations of horseradish peroxidase–catalyzed degradation of single-walled carbon nanotubes. *J Am Chem Soc* 2009;131:17194–17205.
34. Shvedova AA, Tkach AV, Kisin ER, Khaliullin T, Stanley S, Gutkin DW, Star A, Chen Y, Shurin GV, Kagan VE, *et al.* Carbon nanotubes enhance metastatic growth of lung carcinoma via up-regulation of myeloid-derived suppressor cells. *Small* 2013;9:1691–1695.
35. Mercer RR, Scabilloni J, Wang L, Kisin E, Murray AR, Schwegler-Berry D, Shvedova AA, Castranova V. Alteration of deposition pattern and pulmonary response as a result of improved dispersion of aspirated single-walled carbon nanotubes in a mouse model. *Am J Physiol Lung Cell Mol Physiol* 2008;294:L87–L97.
36. Trott O, Olson AJ. Autodock Vina: improving the speed and accuracy of docking with a new scoring function, efficient optimization, and multithreading. *J Comput Chem* 2010;31:455–461.
37. Maynard AD, Baron PA, Foley M, Shvedova AA, Kisin ER, Castranova V. Exposure to carbon nanotube material: aerosol release during the handling of unrefined single-walled carbon nanotube material. *J Toxicol Environ Health A* 2004;67:87–107.
38. Han SG, Andrews R, Gairola CG, Bhalla DK. Acute pulmonary effects of combined exposure to carbon nanotubes and ozone in mice. *Inhal Toxicol* 2008;20:391–398.
39. Han JH, Lee EJ, Lee JH, So KP, Lee YH, Bae GN, Lee SB, Ji JH, Cho MH, Yu IJ. Monitoring multiwalled carbon nanotube exposure in carbon nanotube research facility. *Inhal Toxicol* 2008;20: 741–749.
40. Pauluhn J. Multi-walled carbon nanotubes (baytubes): approach for derivation of occupational exposure limit. *Regul Toxicol Pharmacol* 2010;57:78–89.
41. Driscoll KE, Costa DL, Hatch G, Henderson R, Oberdorster G, Salem H, Schlesinger RB. Intratracheal instillation as an exposure technique for the evaluation of respiratory tract toxicity: uses and limitations. *Toxicol Sci* 2000;55:24–35.
42. Ge C, Du J, Zhao L, Wang L, Liu Y, Li D, Yang Y, Zhou R, Zhao Y, Chai Z, *et al.* Binding of blood proteins to carbon nanotubes reduces cytotoxicity. *Proc Natl Acad Sci USA* 2011;108:16968–16973.
43. Kapralov AA, Feng WH, Amoscato AA, Yanamala N, Balasubramanian K, Winnica DE, Kisin ER, Kotchey GP, Gou P, Sparvero LJ, *et al.* Adsorption of surfactant lipids by single-walled carbon nanotubes in mouse lung upon pharyngeal aspiration. *ACS Nano* 2012;6:4147–4156.
44. Nel A, Xia T, Madler L, Li N. Toxic potential of materials at the nanolevel. *Science* 2006;311:622–627.
45. Lynch I, Salvati A, Dawson KA. Protein–nanoparticle interactions: what does the cell see? *Nat Nanotechnol* 2009;4:546–547.
46. Nel AE, Madler L, Velegol D, Xia T, Hoek EM, Somasundaran P, Klaessig F, Castranova V, Thompson M. Understanding biophysicochemical interactions at the nano–bio interface. *Nat Mater* 2009;8:543–557.
47. Mahmoudi M, Lynch I, Ejtehadi MR, Monopoli MP, Bombelli FB, Laurent S. Protein–nanoparticle interactions: opportunities and challenges. *Chem Rev* 2011;111:5610–5637.
48. Shim M, Kam NWS, Chen RJ, Li YM, Dai HJ. Functionalization of carbon nanotubes for biocompatibility and biomolecular recognition. *Nano Lett* 2002;2:285–288.